



Article

# PLC Implementation and Dynamics of a V/Heart-Shape Chaotic System

Abdul-Basset A. Al-Hussein <sup>1</sup>, Fadhil Rahma Tahir <sup>1</sup>, Hamzah Abdulkareem Abbood <sup>1</sup>, Mazin Majid Abdulnabi <sup>1</sup> and Viet-Thanh Pham <sup>2</sup>,\*

- Department of Electrical Engineering, University of Basrah, Basrah 61001, Iraq; abdulbasset.jasim@uobasrah.edu.iq (A.-B.A.A.-H.); fadhil.rahma@uobasrah.edu.iq (F.R.T.); hamzah.abod@uobasrah.edu.iq (H.A.A.); mazin.abdulnabi@uobasrah.edu.iq (M.M.A.)
- Faculty of Electronics Technology, Industrial University of Ho Chi Minh City, Ho Chi Minh City 70000, Vietnam
- \* Correspondence: phamvietthanh@iuh.edu.vn

#### **Abstract**

This paper investigates the nonlinear dynamics behavior and practical realization of a V/Heart-shape chaotic system. Nonlinear analysis contemporary tools, including bifurcation diagram, Lyapunov exponents, phase portraits, power spectral density (PSD) bicoherence, and spectral entropy (SE), are employed to investigate the system's complex dynamical behaviors. To discover the system's versatility, two case studies are presented by varying key system parameters, revealing various strange attractors. The system is modeled and implemented using an industrial-grade programmable logic controller (PLC) with structured text (ST) language, enabling robust hardware execution. The dynamics of the chaotic system are simulated, and the results are rigorously compared with experimental data from laboratory hardware implementations, demonstrating excellent agreement. The results indicate the potential usage of the proposed chaotic system for advanced industrial applications, secure communication, and dynamic system analysis. The findings confirm the successful realization of the V-shape and Heart-shape Chaotic Systems on PLC hardware, demonstrating consistent chaotic behavior across varying parameters. This practical implementation bridges the gap between theoretical chaos research and real-world industrial applications.

**Keywords:** V/Heart-shape chaotic model; dynamics analysis; PLC; experimental validation; PSD; bicoherence; SE



Academic Editor: Rami Ahmad El-Nabulsi

Received: 13 August 2025 Revised: 22 September 2025 Accepted: 25 September 2025 Published: 1 October 2025

Citation: Al-Hussein, A.-B.A.; Tahir, F.R.; Abbood, H.A.; Abdulnabi, M.M.; Pham, V.-T. PLC Implementation and Dynamics of a V/Heart-Shape Chaotic System. *Dynamics* **2025**, *5*, 40. https://doi.org/10.3390/dynamics5040040

Copyright: © 2025 by the authors. Licensee MDPI, Basel, Switzerland. This article is an open access article distributed under the terms and conditions of the Creative Commons Attribution (CC BY) license (https://creativecommons.org/licenses/by/4.0/).

#### 1. Introduction

Chaotic nonlinear systems have been drawing increasing attention and have become one of the most prominent scientific topics. Because of their numerous and vital applications in a wide range of fields, they are now significantly important in modern engineering and physics [1]. They seem disorganized and may be distinguished by their unpredictable behavior. Their behavior initially appears random, but in fact, it follows a precise and complex evolution. These systems are extremely sensitive to changes in the initial states, where even little modifications to the initial conditions can have a significant effect on the final evolution of the chaotic flow. This phenomenon is known commonly as the butterfly effect. For engineers and scientists working with real-world industrial systems, this sensitivity can be a critical challenge and at the same time a powerful tool, depending on how its handled [2].

Dynamics 2025, 5, 40 2 of 20

The wide range of applications for chaotic nonlinear systems makes their research essential. They cover a wide range of topics, including physics, data encryption, engineering, medicine, and the way our hearts beat. In particular, chaotic systems are used in medicine to investigate biological patterns like heart rhythms [3] and neural activity [4]. On the other hand, chaotic models are used in engineering applications to improve the functionality of technology and design sophisticated control methods [5]. Additionally, these systems have demonstrated effectiveness in the advancement of modern encryption methods, providing high degrees of data transmission security [6,7]. It is also worth noting that, while these applications are compelling, real-world implementation often involves trade-offs between complexity, cost, and stability. Modern tools and computational software offer tremendous opportunities to study chaotic systems and explore their future applications.

The realization of chaotic systems initially relied on discrete components such as comparators, diodes, capacitors, and operational amplifiers. These analog circuits elements provide a way to generate chaotic dynamics by emulating nonlinear system behavior. However, such implementations were inherently limited by their low-frequency response, which restricted their application in high-speed systems [8]. Moreover, analog components are susceptible to noise, aging, and environmental factors, which can lead to inconsistencies in system performance over time. Due to the previously discussed issues, recently, many chaotic systems have been implemented using digital element circuitry.

The usage of digital components has revolutionized the realization and implementation of nonlinear chaotic models, where digital platforms offer significant advantages, including high-speed operation, precise control, and reconfigurability. Additionally, digital implementations are less affected by environmental variations and provide greater stability, unlike analog systems circuitry. Moreover, they enable the design and simulation of complex chaotic systems with higher accuracy, rendering them suitable for applications such as secure communications, random number generation, and encryption algorithms. The flexibility and scalability of digital framework designs allow researchers to test various chaotic models and adapt systems as needed, paving the way for advancements in fields like cryptography and nonlinear dynamics studies [9].

The study in [10] explores a novel 3D chaotic mechanical jerk and details an FPGAbased implementation of the system, where discrete equations derived through numerical methods are synthesized. By optimizing hardware through pipeline operations, the FPGA design achieves efficient resource utilization. The work in [11] enhances a chaotic system build using a memristive and the inclusion of a transcendental nonlinearities using fractional-order mathematical derivation. The FPGA implementation focuses on integrating a reconfigurable coordinate rotation digital computer (CORDIC) for trigonometric and hyperbolic function calculation and realizes the fractional-order operators through the Grünwald-Letnikov (GL) definition. The system was realized on the Artix-7 FPGA kit, providing a high throughput of 0.396 Gbit/s. The researcher in [12] introduced a six-dimensional chaotic memristor system with hidden attractors. Simulations on a DSP platform validated its accuracy, highlighting its potential for secure communication and image encryption applications. A four-dimensional chaotic system with rich dynamics, including attractor coexistence, was implemented using DSP chip F28335. The continuous system was discretized using the Runge-Kutta method and implemented efficiently. A DAC8552 converted digital outputs analog signals for visualization, with experimental results aligning with simulations. The system shows promise for secure communication and image encryption [13].

While most existing research focuses on FPGAs and DSPs, PLCs (programmable logic controllers) offer unique advantages, such as their robustness, ease of integration into industrial environments, and widespread use in automation. PLC devices can be considered

Dynamics 2025, 5, 40 3 of 20

the backbone of the modern industrial automation. They were originally developed to replace traditional relay-based automatic control systems. But due to their modular design, real-time processing capabilities, and ability to integrate with industrial networks and their easy integration to a wide range of sensors and actuators, PLCs became very crucial for industrial applications [14]. Moreover, the computational power and flexibility of PLC devices can be employed to precisely realize, implement, and control chaotic systems in a powerful way. Chemical processing facilities can use PLC-based chaotic control mechanisms to manage sensitive reactions and achieve peak performance even when external factors like temperature and pressure fluctuate. Another significant application of PLCs lies in robotics, motion control, and ball mill [15]. For instance, chaotic trajectories can be utilized to navigate complex environments, avoiding obstacles and optimizing paths in real time [16]. Energy usage and load balancing are common challenges for industrial operations. Therefore, another area where PLCs and chaotic systems work remarkably well together is energy management. The PLC implementation of chaotic-based algorithms can be used to optimize energy distribution by avoiding waste and dynamically adapting to shifting demands. Significant cost savings result from this, and it also supports international initiatives to lower carbon emissions and advance sustainable practices [17]. The Industrial Internet of Things (IIoT) provides global connectivity between components in different locations and technological advancement that leads to the implementation of Industry 4.0 [18]. Chaotic systems provide robust signal transmission, while PLCs ensure seamless integration with other IIoT platforms, enabling predictive maintenance and realtime decision-making. PLCs can seamlessly integrate power line communication systems with other industrial automation networks, such as SCADA or IoT-based frameworks. This enables centralized control and monitoring of the communication system while maintaining data security and integrity.

This paper introduces an experimental implementation of the V-shape/Heart-shape chaotic system. It gets its name from the fact that this chaotic dynamical model displays two different typologies of strange attractors based on the values of its parameters. Numerical methods are used to investigate both dynamical behaviors in these two cases. This paper's second goal is to make use of an industrial-type PLC, the XEC-DN32H device from the LS XGB family, to implement the differential equation of the presented chaotic model. The programmable hardware allows the experimental characterization of the system dynamics with a reconfigurable and rapid experimental setup. Studying chaotic systems using PLCs would also provide valuable insights into their practical utility in real-world scenarios. Unlike FPGAs and DSPs, PLCs are already integrated into many industrial operations, which could simplify the adoption of chaos-based solutions. Furthermore, such research could expand the functionality of PLCs beyond their traditional role in deterministic control systems, enabling industries to benefit from the unique properties of chaos, such as sensitivity to initial conditions and pseudo-random behavior. The novelty of this work lies in demonstrating that chaotic systems can be successfully implemented on PLC hardware, highlighting the potential of PLCs not only as control devices but also as platforms for advanced computational and security-related applications. This underexplored direction opens promising opportunities for innovation, particularly in industrial networking environments such as SCADA and IIoT systems, where PLCs are already essential components. By highlighting this perspective, our study not only presents a novel implementation but also opens a promising pathway for future research and applications. The remaining parts of this paper are organized as follows. In Section 2, the dynamic properties of the proposed V/Heart-shape chaotic system are analyzed, highlighting its nonlinear characteristics and parameter-dependent behaviors. Section 3 describes the detailed methodology for realizing the chaotic system using a high-performance programmable logic controller (PLC) device. Dynamics 2025, 5, 40 4 of 20

The design employs the usage of user-defined function blocks programmed in ST language. Section 4 discusses the experimental results obtained from both simulation and real-time hardware testing, demonstrating the system's ability to generate complex self-excited attractors. Finally, Section 5 concludes the paper by summarizing the key findings and outlining potential directions for future research.

# 2. Dynamic Properties of the V/Heart-Shape Chaotic System

The primary step in integrating chaotic systems with PLCs is developing a mathematical model that accurately represents the system's dynamics. This section introduces the V/Heart-shape chaotic system, which is a multi-scroll attractor. The multi-scroll attractor is proven to have better properties, like having higher entropy for random number generation, compared to normal attractors. The dimensionless state equations of the presented V/Heart-shape chaotic model are given as follows [19]:

$$\begin{cases} \dot{X} = Y - X, \\ \dot{Y} = sign(X)[1 - m_1 Z + G(Z)], \\ \dot{Z} = |X| - m_2 Z \end{cases}$$
 (1)

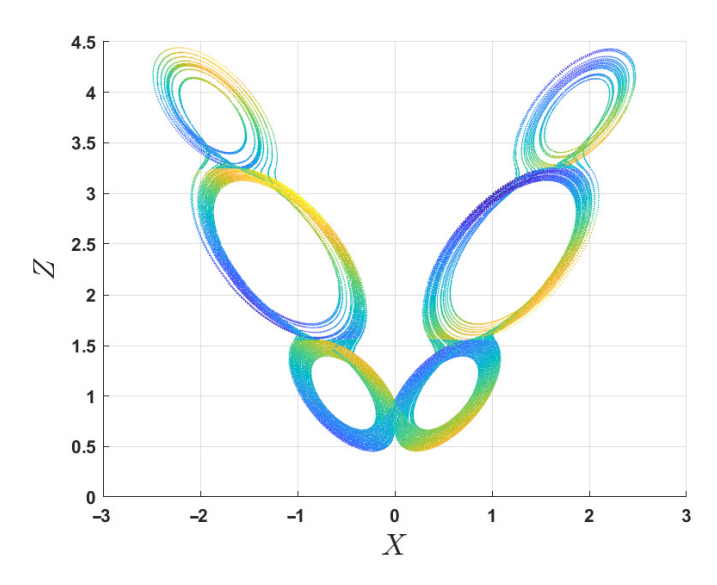
$$G(z) = \begin{cases} 0 & Z < s_0 \\ d_1 & s_0 \le Z < s_1 \\ \vdots & \vdots \\ d_{N-1} & Z \ge s_{N-1} \end{cases}$$
 (2)

where  $d_i$  is the additive coefficient, and  $s_i$  is the limiting coefficient.  $m_1$  and  $m_2$  are system parameters. G(z) is the introduced piecewise nonlinear staircase function used to generate the multi-scrolls, and the number of scrolls of the attractor is 2N. Parameters  $d_i$  and  $s_i$  in (2) control the scrolls' diameter and height characteristics, respectively.

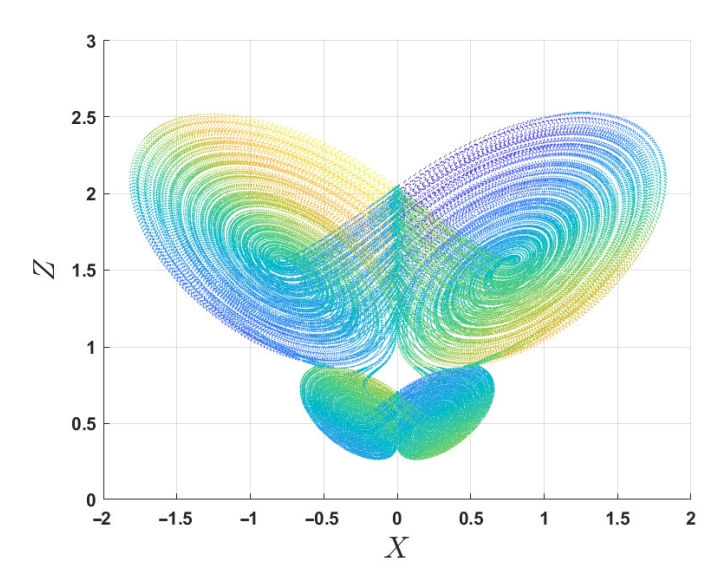
To thoroughly explore the dynamics of the presented chaotic system, we will investigate it under two distinct sets of parameters. Initially, we will analyze the system when parameter  $m_1$  is set to 1. This specific configuration will allow us to observe the baseline behavior and inherent chaotic properties of the system. Subsequently, we will modify parameter  $m_1$  to 2 and repeat the analysis. This change is expected to alter the system's behavior, potentially leading to different dynamical features. By evaluating the results from the two parameter sets, the aim is to understand how varying control parameter  $m_1$  influences the chaotic nature of the system. Such comparative analysis will highlight the sensitivity of the system to parameter changes and provide insights into its stability and bifurcation behavior. Through this thorough analysis, a deeper understanding of the underlying mechanisms driving the chaotic behavior and the impact of parameter variations on the system's dynamics can be gained.

Figure 1 shows the V-shape self-excited adjacent parabolic loop attractor. This strange attractor generated from the presented chaotic system with N=3 scrolls, when  $m_1=1$  and the initial values are selected as  $[X_0,Y_0,Z_0]=[0.1,0.5,0.6]$ . A family of interconnected Heart-shape self-excited attractors are produced by setting parameter  $m_1=2$ , as shown in Figure 2 with N=2 and initial condition  $[X_0,Y_0,Z_0]=[0.1,0.5,0.6]$ .

Dynamics 2025, 5, 40 5 of 20



**Figure 1.** Phase portrait projection of V-shape attractor for system (1) when  $m_1 = 1$ .



**Figure 2.** Phase portrait projection of heart-shape attractor for system (1) when  $m_1 = 2$ .

To analyze the employed chaotic system dynamical behavior, various state-of-the-art nonlinear analysis tools can be utilized, each serving a distinct purpose. Bicoherence is a powerful tool that measures quadratic phase coupling between different frequency components of a signal, helping to identify nonlinear interactions even in noisy data. This is particularly useful in distinguishing chaotic behavior from quasi-periodic phenomena. Power spectral density (PSD), on the other hand, analyzes the frequency content of a signal. In chaotic systems, PSD typically reveals a broadband spectrum, indicating a wide range of frequencies, which helps differentiate chaotic signals from noise and periodic signals. The PSD and bicoherence of system (1) with system parameters  $m_1 = 1$  and  $m_1 = 2$  are given in Figures 3 and 4, respectively. These figures indicate the broadband nature and the nonlinearity strength of the suggested chaotic system.

Dynamics 2025, 5, 40 6 of 20

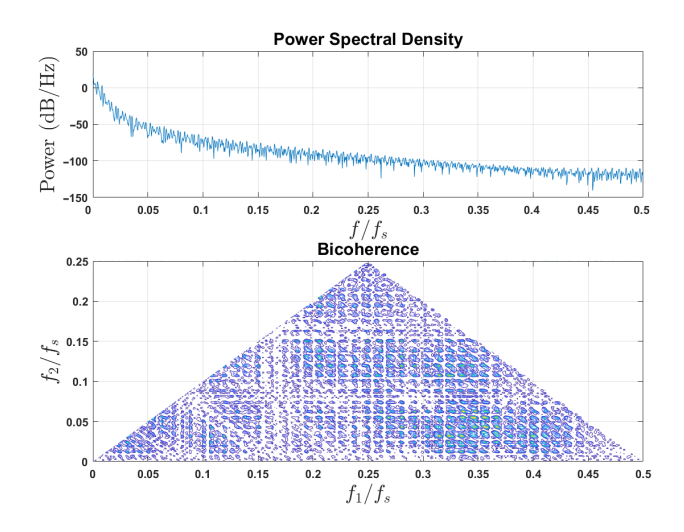


**Figure 3.** Bicoherence and PSD plot for system (1) at  $m_1 = 1$ .

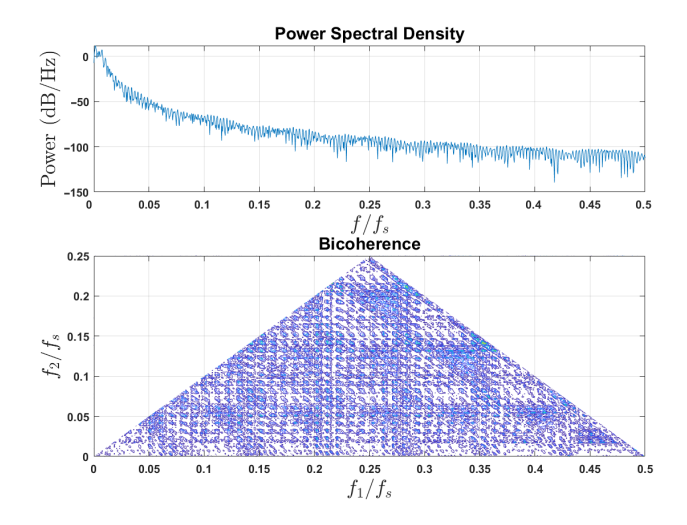


**Figure 4.** Bicoherence and PSD plot for system (1) at  $m_1 = 2$ .

A Poincaré map is another essential and important tool that can be used to reduce the phase space dimension of a dynamical system by considering a cross-section in its phase space. This technique aids in visualizing the long-term behavior of a system and identifying periodic orbits, fixed points, and chaotic regions in a straightforward manner [20]. Bifurcation diagrams provide insights into how the qualitative behavior of a system changes as a parameter varies. These diagrams are crucial for identifying transitions between periodic and chaotic states, thereby understanding the stability and dynamics of the system. Lyapunov exponents measure the rate of separation of infinitesimally close trajectories within the system. Positive Lyapunov exponents are indicative of chaos, reflecting the system's sensitivity to initial conditions, which is a hallmark of chaotic behavior. Together, these tools offer a comprehensive framework for analyzing, predicting, and potentially controlling chaotic systems, thus providing a deep understanding of their intricate dynamics.

Poincaré maps for both the  $m_1 = 1$  and  $m_1 = 2$  cases, projected onto the Y = 0 plane, are depicted in Figure 5 and Figure 6, respectively. To analyze and verify the chaotic behavior of the system, for both cases, the intersections of the system trajectories with the Y = 0 plane provide a sequence of points that form the Poincaré map. In both contexts of  $m_1 = 1$  and  $m_1 = 2$ , the maps may reveal chaotic behavior where the points are organized in regular patterns, such as distinct clusters or closed curves.

Dynamics 2025, 5, 40 7 of 20

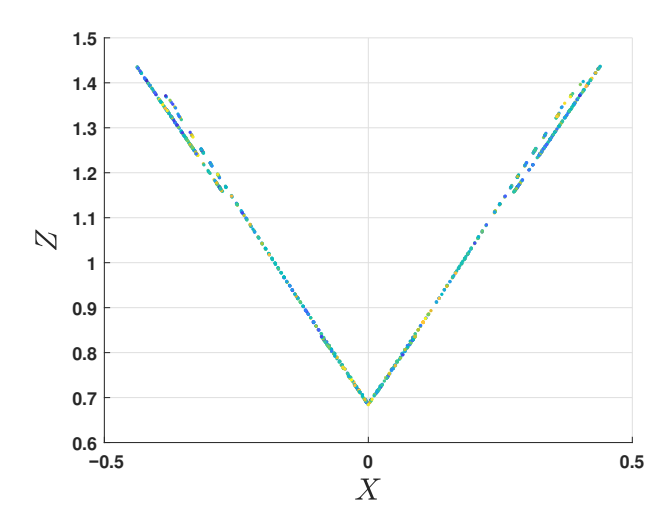


**Figure 5.** Poincaré map in the (X - Z) cross-section at the Y = 0 plane of system (1) when  $m_1 = 1$ .

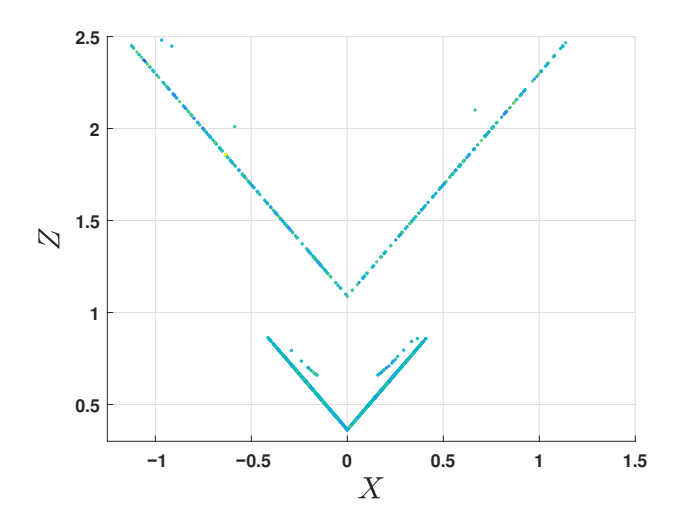


**Figure 6.** Poincaré map in the (X - Z) cross-section at the Y = 0 plane of system (1) when  $m_1 = 2$ .

The bifurcation diagram of the system for control parameter  $m_2$ , as depicted in Figures 7 and 8, provides a clear visualization of the system's dynamic behavior as parameter  $m_2$  is increased. With the initial conditions set at [0.5, 0.5, 0.5] for the initial iteration, and reinitializing to the last values of the state variables, the plots show how the system evolves under forward continuation. The plots reveal a complex dynamic, characterized by transitions between different states. Notably, there are regions where the plot exhibits a dense, seemingly random pattern, indicating the presence of chaotic behavior. Thus, the bifurcation plot not only confirms the existence of chaos but also highlights the intricate structure of the system's phase space under varying parameter conditions.

The analysis of system (1)'s dynamics through the Lyapunov exponents and bifurcation diagram reveals a strong correlation between the two tools in identifying chaotic regions. Lyapunov exponents quantify the rate of separation of infinitesimally close trajectories in a dynamical system, providing a direct measure of the system's sensitivity to initial conditions. In particular, a positive Lyapunov exponent indicates exponential divergence of nearby trajectories, which is a intrinsic feature of chaotic dynamics behavior.

Dynamics 2025, 5, 40 8 of 20

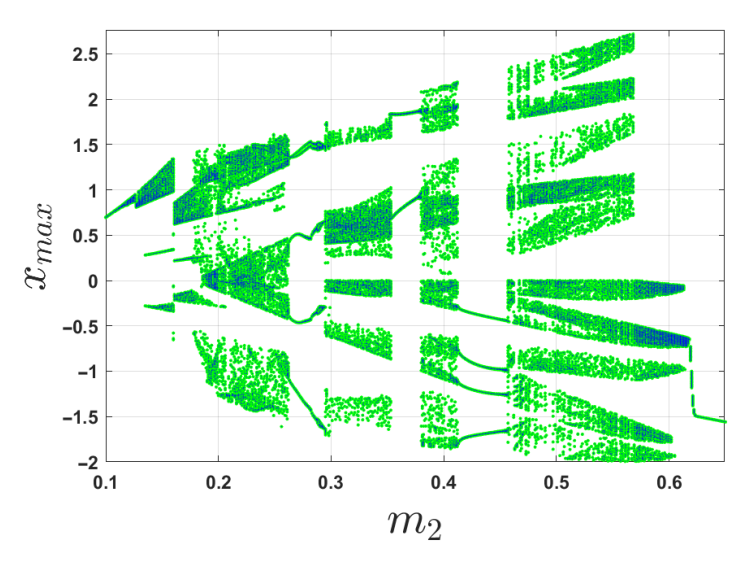


**Figure 7.** Bifurcation diagram of system (1) with respect to parameter  $m_2$  and fixed value of  $m_1 = 1$ , based on forward continuation method.

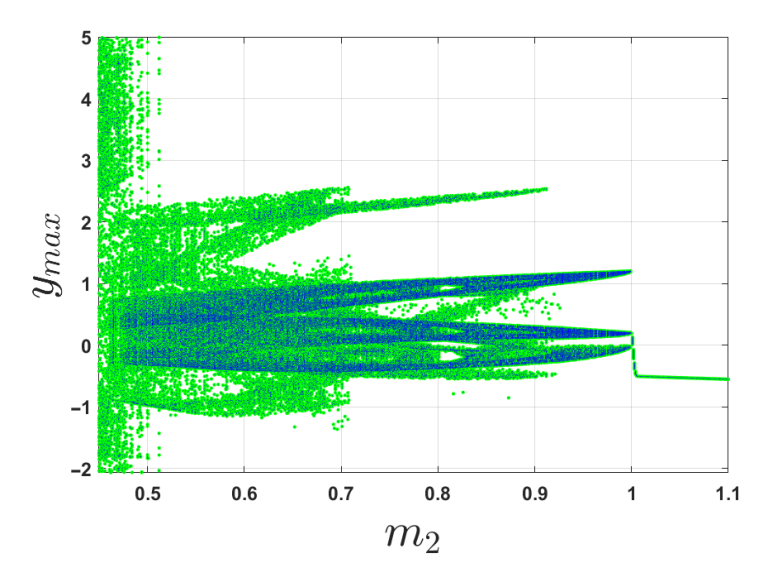


**Figure 8.** Bifurcation diagram of system (1) with respect to parameter  $m_2$  and fixed value of  $m_1 = 2$ , based on forward continuation method.

When comparing the plot of the Lyapunov exponents with the bifurcation diagram, regions of chaotic behavior correspond to those where the largest Lyapunov exponent becomes positive. In the bifurcation diagram, chaotic regions are typically characterized by dense, irregular distributions of points, indicating a loss of periodicity. The Lyapunov exponent plot complements this by quantitatively confirming these chaotic regions; positive exponents are observed precisely in the parameter ranges where the bifurcation diagram suggests chaotic dynamics.

This alignment is not coincidental but rather a reflection of the underlying nonlinear dynamics of the system. While the bifurcation diagram provides a qualitative visualization of the transitions in system behavior as the control parameter varies, the Lyapunov exponent plot offers a quantitative measure of the stability or instability of those behaviors. These two methods, when combined, can offer an in-depth understanding of the dynamics of the system. This duality emphasizes how crucial it is to combine the two methods when validating and interpreting complicated dynamical behaviors. Strong evidence of chaos is provided by the occurrence of positive Lyapunov exponents in particular parameter ranges, which supports the inferences made from the bifurcation diagram. This methodical

Dynamics 2025, 5, 40 9 of 20

approach demonstrates the strength of integrating qualitative and quantitative techniques for the analysis of nonlinear dynamical systems.

Lyapunov exponents (LEs) for the V/Heart shape system are derived using A. Wolfs' method [21] for 10,000 s to check the chaotic state of the system for different system parameter values. Figure 9 shows the Lyapunov exponent (LE) spectrum for the system parameter in the range  $m_2 \in [0.45, 1.1]$ , and it is clear that for  $m_2 \in [0.45, 1)$ , the largest exponent remains positive, which is a conclusive indicator of chaotic dynamics within this parameter range. Positive Lyapunov exponents imply that small perturbations in the initial conditions grow exponentially over time, leading to sensitive dependence on initial conditions—a hallmark of chaos.

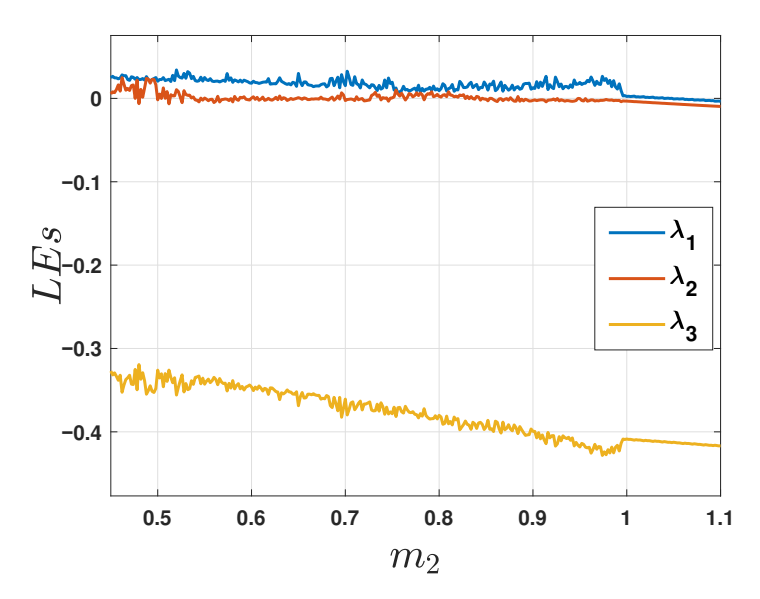


**Figure 9.** Lyapunov diagram for system (1), with respect to parameter  $m_2$  and a fixed value of  $m_1 = 2$ .

Spectral entropy (SE) is an important tool in studying chaotic systems because it provides a quantitative measure of the system's complexity. In chaotic states, the spectrum spreads over a wide frequency range, producing higher SE. This makes SE a useful tool for detecting transitions from order to chaos and evaluating the degree of unpredictability in the system. Furthermore, SE serves as a valuable feature in applications such as random sequence generation and the classification of nonlinear dynamical behaviors. It can be briefly defined as follows [22]:

$$Y(k) = \sum_{n=0}^{N-1} y(n)e^{-\frac{j2\pi nk}{N}} = \sum_{n=0}^{N-1} y(n)W_N^{nk},$$
(3)

In Equation (3), y(n)(n = 0, 1, 2 ... N - 1) is the chaotic sequence generated by the second variable of the presented V/Heart-shape model after removing the DC component, and Y(k)(k = 0, 1, 2 ... N - 1) is the corresponding discrete Fourier transform of y(n)(n = 0, 1, 2 ... N - 1). Using Paserval's theorem, the power spectrum at any particular frequency can be calculated using the first half of the discrete sequence Y(k)(k = 0, 1, 2 ... N/2 - 1) as it has a symmetrical property:

$$p(k) = \frac{1}{N} |Y(k)|^2 \tag{4}$$

and the total power spectrum can be described as

$$p_{tot}(k) = \frac{1}{N} \sum_{k=0}^{\frac{N}{2}-1} |Y(k)|^2$$
 (5)

Dynamics **2025**, 5, 40

Then, the probability of the relative power spectrum  $p_k$  can be written as  $p(k)/p_{\text{tot}}(k)$  through the combination of Equations (4) and (5). Spectral entropy, according to the Shannon entropy principle, is equal to the sum of  $p_k \ln(1/p_k)(k=0,1,2...N/2-1)$ . The final value of the spectral entropy approach to  $\ln(N/2)$  is well known; therefore, the normalized spectral entropy can be obtained as follows (6):

$$SE = \frac{-\sum_{k=0}^{\frac{N}{2}-1} p_k \ln p_k}{\ln(N/2)}$$
 (6)

The aforementioned derivation shows that a larger SE value suggests a more complex oscillation for a single chaotic system; conversely, a smaller SE value indicates a more obvious oscillation for a single chaotic system. As a result, we think that various SE values ought to correlate with various chaotic system states.

As presented in Figure 10, the SE complexity values of system (1) fluctuate around high values for  $m_2 \in [0.45, 1]$ , which is low for  $m_2 \in (1, 1.1]$ . Therefore, the result in Figure 10 is consistent with the bifurcation diagram in Figure 8 and that of the Lyapunov exponents in Figure 9.

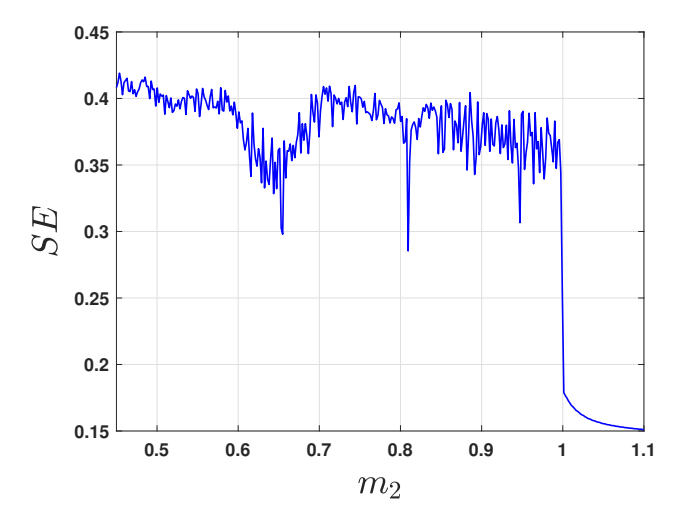


**Figure 10.** Spectral entropy complexity diagram of system (1) with  $m_2$  varying from 0.45 to 1.1, and a fixed value of  $m_1 = 2$ .

Important measures indicate the usefulness of the proposed chaotic system for use in encryption algorithms such as histogram and autocorrelation analysis. Figure 11 shows the histogram plot of the generated chaotic sequence from the presented V/Heart-shape model (1), which is non-uniformly distributed and can lead to low contrast. And in security applications, it may provide clues for cryptanalysis. To further enhance the security of the generated sequence, the histogram equalization procedure is used. Histogram equalization is a technique used to enhance the sequence contrast by redistributing the values to create a more uniform, or "flatter," histogram. The proposed histogram equalization procedure is given as follows [23,24]:

$$y_{new} = (Round(y_{old} * N_1)) mod(N_2)$$
(7)

where  $N_1$  is a large number, chosen to be  $10^5$  in this paper, and  $N_2$  is selected to be 250. The histogram and autocorrelation plots for the new generated sequence are given in Figure 12 and Figure 13, respectively. The two figures show that the presented chaotic system behaves similar to random time-series, which is useful for chaotic encryption application in industrial fields.

Dynamics 2025, 5, 40 11 of 20

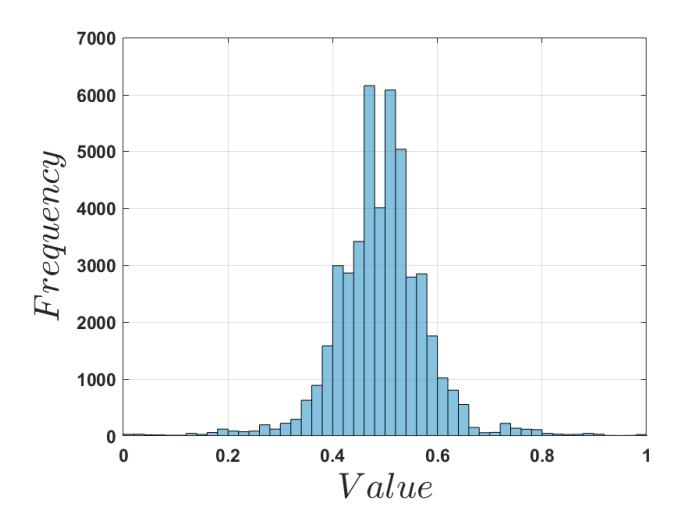


**Figure 11.** Histogram for the original sequence generated by system (1) when  $m_1 = 2$ .

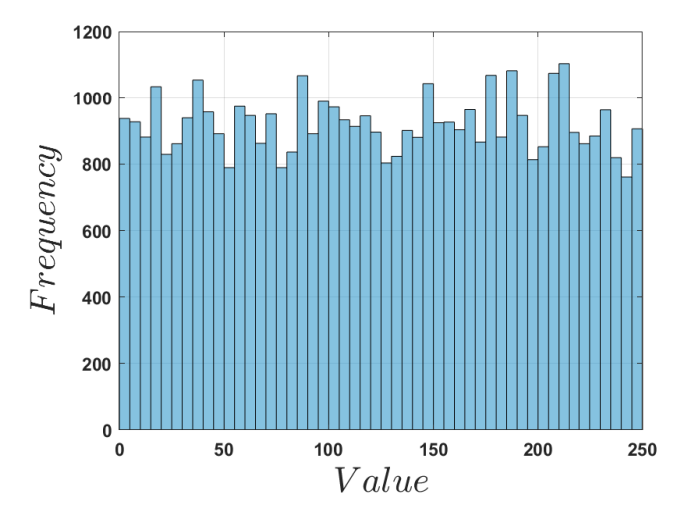


**Figure 12.** Histogram result for the chaotic sequence generated by system (1) when  $m_1 = 2$ , after applying the proposed histogram equalization algorithm.

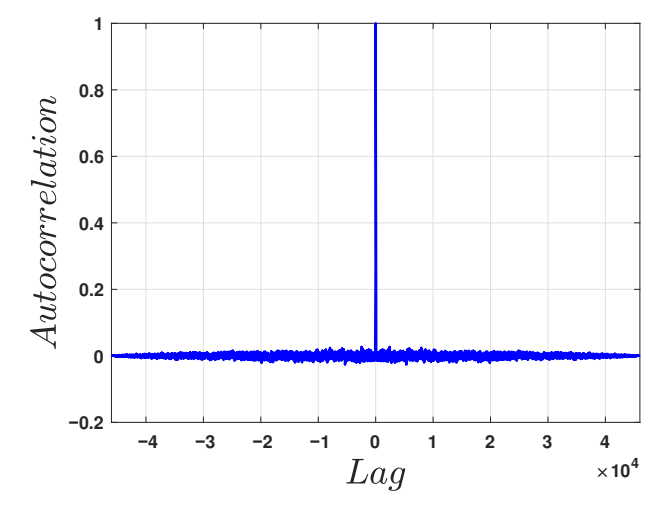


**Figure 13.** Autocorrelation result for the chaotic sequence generated by system (1) when  $m_1 = 2$ , after applying the proposed histogram equalization algorithm.

Dynamics **2025**, 5, 40

# 3. PLC Implementation of the V/Heart-Shape Chaotic System

Programmable logic controllers are specialized computers made especially for industrial applications. Their architecture is designed to process and regulate complicated industrial processes in real time by handling a large number of input and output (I/O) signals. The core components of a PLC include the Central Processing Unit (CPU), which executes control programs; memory, which stores these programs and data; input and output connection sections for interfacing with sensors, actuators, and other external devices; the power unit, which supplies the necessary electrical power; and the communication interface section, which allows the PLC to communicate with other devices and systems. Additionally, the programming device is used to create, edit, and download control programs into the PLC [25,26].

## 3.1. PLC Hardware Setup

In the development of the chaotic model, the LS XG5000 version 4.78 programming environment was utilized, employing structured text (ST) language for coding the V/Heartshape chaotic model. This choice of software and language ensures precise control and flexibility in modeling complex chaotic systems. To implement the continuous-time equations in (1), it should be converted into discrete-time versions suitable for programming on PLCs using the Runge–Kutta 4 numerical method. The presented chaotic model was achieved using an LS XGB XEC-DN32H compact PLC, which was provided by a digitalto-analogue converter expansion module (XBF-DV04A). This module has a (0  $\,
ightarrow\,$  10 V) dynamics output range, and  $(0 \rightarrow 4000)$  as the input range. A more technical specification of the used PLC and analogue output expansion module is given in Table 1 and Table 2, respectively. This setup allows the PLC to accurately convert analog signals into digital form, which is essential for processing and controlling chaotic signals. The combination of advanced software tools and robust hardware components demonstrates the capability of PLCs to handle sophisticated control tasks in real-time industrial environments. This integration of chaos theory into industrial automation highlights the innovative potential of PLCs in managing complex systems and processes.

Table 1. LS XGB XEC-DN32H high-performance compact PLC specifications [27].

Specification	Details
Power Supply	AC 110–240 V-AC main supply
Input/Output	18 DC 24 V inputs; 18 transistor (source-type) outputs
Processing Speed	83 ns/step
Scan Cycle	0.5–1 ms
Program Capacity	15 K steps or approximately 200 KB
Max I/O Expansion	Up to 10 expansion modules; up to 352 total I/O points
Communication Ports	USB (Rev 1.1); RS-232C (1 channel, loader); RS-232C/RS-
	485 (2 channels)
<b>Built-in Functionalities</b>	Pulse catch; input filter; external interrupt; PID control;
	high-speed counter; positioning; RTC
Programming Standards	IEC-61131-3 languages supported (LD, SFC, ST)

Dynamics 2025, 5, 40 13 of 20

Specification	Details
Module Type	Analog Output (4-Ch, Voltage)
Output Range	0–10 V DC
Resolution	12-bit
Number of Channels	4
Max Resolution Voltage	2.5 mV
Unsigned Value	0 to 4000
Signed Value	-2000 to 2000
Max Conversion Speed	1 ms/channel
Minimum Load Resistance	$\geq$ 2 k $\Omega$

Table 2. XBF-DV04A digital-to-analogue converter expansion module specifications [28].

#### 3.2. State Variable Mapping and Discretization

Experimental measurements can be carried out through the I/O modules on the PLC. The dynamic range of signals inside the PLC is measured through voltage signals in differential mode. Thus, an equivalent system is designed by assuming that the state variables of the dynamical system are voltage signals. To generate chaotic systems from the PLC processor, the systems must be rescaled in a manner that makes them compatible with the characteristics of the DAC module used. Then, a transformation from continuous-time systems to discrete-time systems has been applied to the rescaling systems.

Suppose a dimensionless, continuous-time chaotic system described in the general form [29] exists:

$$\dot{x}_{1}(t) = f_{1}(x_{1}, x_{2}, \dots, x_{n}) 
\dot{x}_{2}(t) = f_{2}(x_{1}, x_{2}, \dots, x_{n}) 
\vdots 
\dot{x}_{n}(t) = f_{n}(x_{1}, x_{2}, \dots, x_{n})$$
(8)

Here,  $\mathbf{L_{1j}} \leq \mathbf{x}_j \leq \mathbf{L_{2j}}$ ,  $j = 1, 2, 3 \dots, n$ . If the range of  $\mathbf{x}_j$  is not compatible with the used PLC digital-to-analogue output module, the XBF-DV04A in this work, then the characteristics of the rescaling process will be set as follows:

$$\mathbf{x}_j = \frac{\mathbf{x}_j}{\mathbf{a}_i} - \mathbf{b}_j \tag{9}$$

where  $(L_{1j} + b_j \ge 0, b_j \ge 0)$  and  $a_j = \frac{4000}{L_{2j} + b_j}$ . By applying these changes, system (8) becomes

$$\dot{X}_{1}(t) = f_{1}\left(\frac{x_{1}}{a_{1}} - b_{1}, \frac{x_{2}}{a_{2}} - b_{2}, \dots, \frac{x_{n}}{a_{n}} - b_{n}\right) * a_{1}$$

$$\dot{X}_{2}(t) = f_{1}\left(\frac{x_{1}}{a_{1}} - b_{1}, \frac{x_{2}}{a_{2}} - b_{2}, \dots, \frac{x_{n}}{a_{n}} - b_{n}\right) * a_{2}$$

$$\vdots$$

$$\dot{X}_{n}(t) = f_{1}\left(\frac{x_{1}}{a_{1}} - b_{1}, \frac{x_{2}}{a_{2}} - b_{2}, \dots, \frac{x_{n}}{a_{n}} - b_{n}\right) * a_{n}$$
(10)

The discrete-time form of Equation (10) is provided using Runge–Kutta 4 with step size h as follows:

Dynamics 2025, 5, 40 14 of 20

$$X_{1}(k+1) = X_{1}(k) + [R_{11} + 2R_{12} + 2R_{13} + R_{14}]/6$$

$$X_{2}(k+1) = X_{2}(k) + [R_{21} + 2R_{22} + 2R_{23} + R_{24}]/6$$

$$\vdots$$

$$X_{n}(k+1) = X_{n}(k) + [R_{n1} + 2R_{n2} + 2R_{n3} + R_{n4}]/6$$
(11)

where

$$R_{i1} = G_i[X_1(k), X_2(k), \dots, X_n(k)]a_ih$$

$$R_{i2} = G_i[X_1(k) + 0.5R_{11}, \dots, X_n(k) + 0.5R_{n1}]a_ih$$

$$R_{i3} = G_i[X_1(k) + 0.5R_{12}, \dots, X_n(k) + 0.5R_{n2}]a_ih$$

$$R_{i4} = G_i[X_1(k) + R_{13}, \dots, X_n(k) + R_{n3}]a_ih$$
(12)

for  $i = 1, 2, 3, \ldots, n$ . The classical fourth-order Runge–Kutta method with a sufficiently small step size was employed in this study to ensure reliability, stability, and preservation of original chaotic dynamics. In future work, we plan to investigate the impact of different numerical integration schemes on the accuracy and stability of chaotic behavior. Such a comparison will help to better assess the numerical reliability of PLC-based realization. Therefore, to design and implement a dynamical system in the PLC, the programming flowchart should be followed, shown in Figure 14.

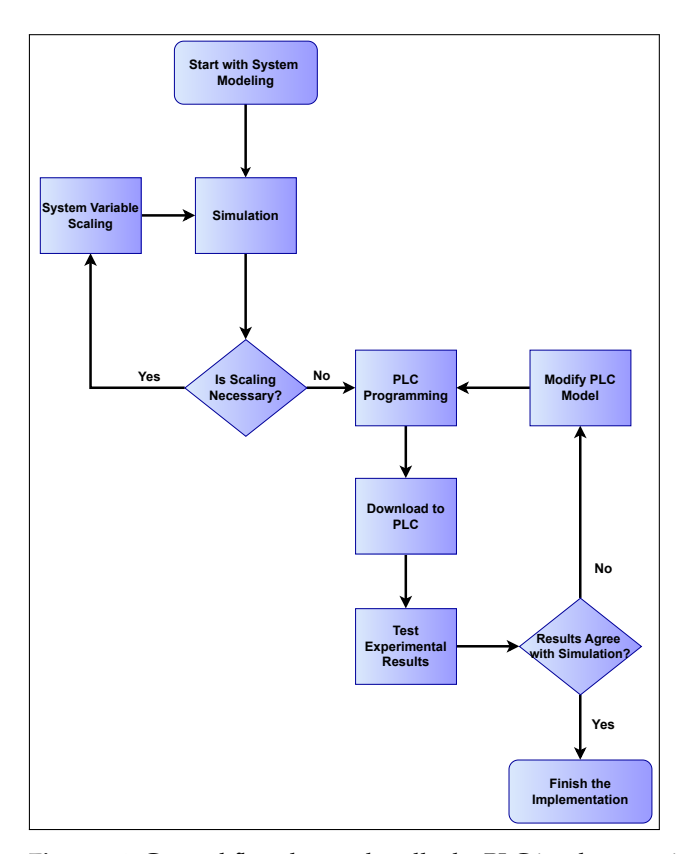


Figure 14. General flowchart to handle the PLC implementation of the chaotic system.

# 4. Implementation Results

The proposed realization of a chaotic system using a PLC platform was experimentally validated through a structured series of software simulations and hardware-based tests. In this work, the three state variables of the chaotic system were implemented as user-defined function blocks (UDFBs), enabling modular and reusable code within the XG5000 version 4.78 programming environment. As illustrated in Figure 15, these UDFBs encapsulate the system's nonlinear differential equations, allowing for the precise and scalable execution of

Dynamics 2025, 5, 40 15 of 20

the chaotic dynamics on the XEC-DN32H. This modular design not only enables real-time execution of the chaotic system on industrial-grade hardware but also facilitates scalable implementation for more complex dynamical models.

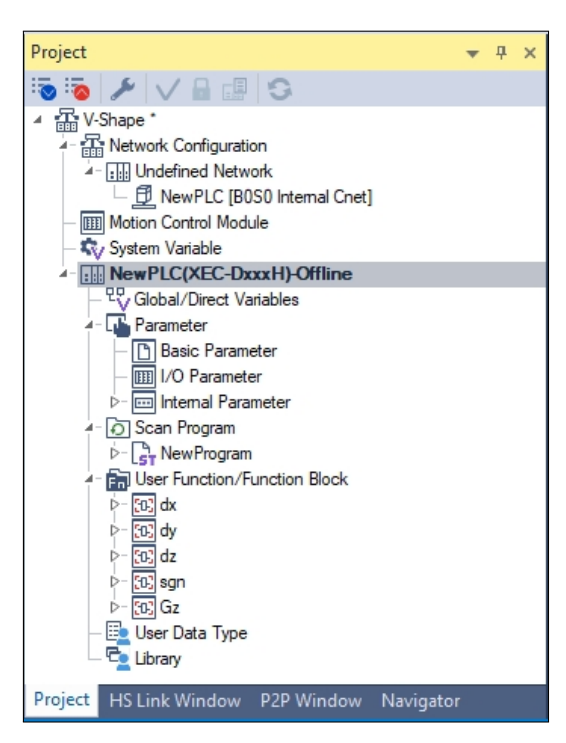
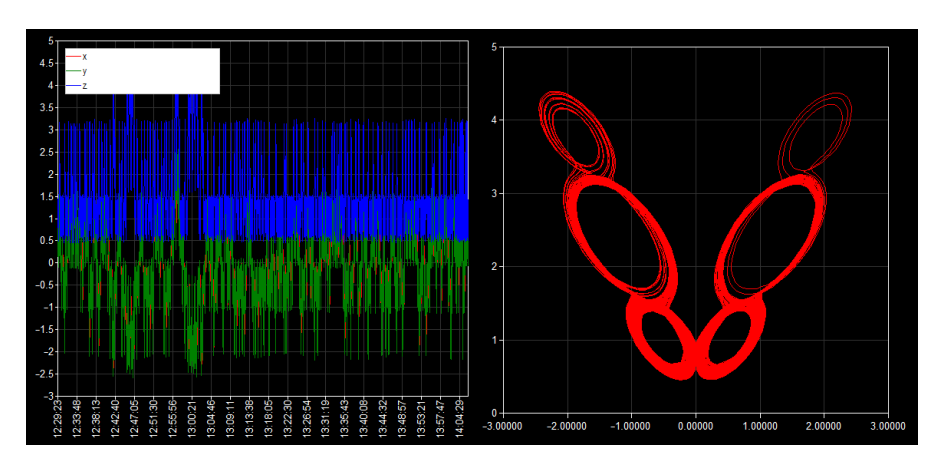


Figure 15. PLC project framework designed to model V/Heart-shape chaotic system (1).

To rigorously validate the correctness and dynamic behavior of the embedded chaotic system, the PLC code was thoroughly tested within the XG5000 software version 4.78 simulation environment. The simulation outputs, presented in Figures 16 and 17, illustrate the state variable trajectories and their corresponding two-dimensional phase portraits for system parameters  $m_1=1$  and  $m_1=2$ , respectively, at an integration step size equal to h=0.005, which provides a suitable balance between numerical accuracy and computational feasibility for the PLC platform. These phase portraits reveal the qualitative behavior of the system's attractors, confirming the successful reproduction of expected chaotic oscillations. The traces demonstrate the system's sensitivity to initial conditions and parameter variations—hallmarks of chaotic behavior—thereby validating the computational accuracy of the PLC implementation before hardware deployment.



**Figure 16.** State variable trend graphs and 2D phase portrait for system (1) when  $m_1 = 1$ .

Dynamics 2025, 5, 40 16 of 20

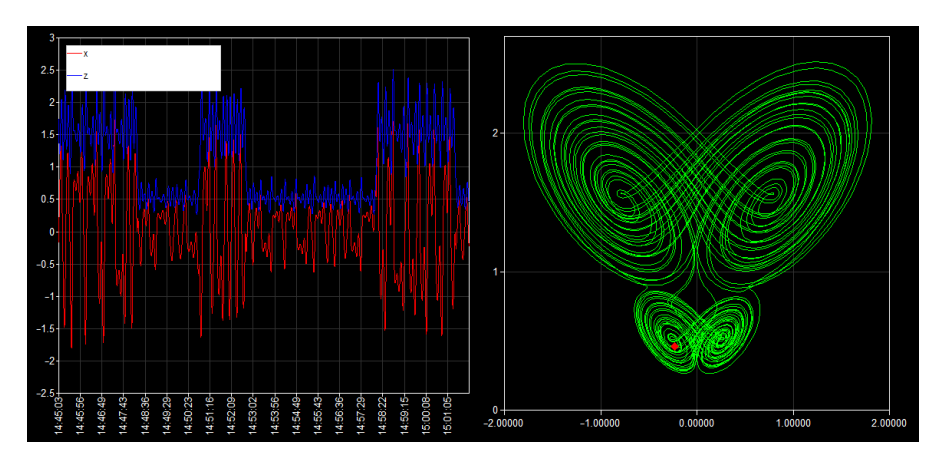


**Figure 17.** State variable trend graphs and 2D phase portrait for system (1) when  $m_1 = 2$ .

Subsequent experimental validation was conducted using the physical setup shown in Figure 18, where the XEC-DN32H PLC, equipped with the XBF-DV04A analogue output module, was interfaced with a digital oscilloscope. This setup enabled real-time monitoring of the chaotic signals generated by the PLC. When the system parameter was set to  $m_1 = 1$  and mapping parameters were set as  $a_1 = a_2 = 750$ ,  $a_3 = 800$ ,  $b_1 = 3$ ,  $b_2 = 2.5$ , and  $b_3 = 1$ , the experimental results shown in Figure 19 exhibit a distinct V-shaped self-excited attractor with adjacent parabolic loops, forming a two-scroll chaotic pattern. The attractor's geometric structure closely matches the simulated phase portrait, indicating a high degree of fidelity between the software simulation and physical system behavior.

Furthermore, by modifying the system parameter to  $m_1 = 2$  and mapping parameters to  $a_1 = 1000$ ,  $a_2 = 800$ ,  $a_3 = 1400$ ,  $b_1 = 3$ ,  $b_2 = 2.5$ , and  $b_3 = 1$ , the chaotic system exhibits a transition in its attractor topology. As shown in Figure 20, the oscilloscope captures a complex family of interconnected heart-shaped loops, corresponding to a three-scroll self-excited attractor. This evolution in the attractor's geometry with respect to the system parameter illustrates the system's nonlinear response and parameter sensitivity, consistent with theoretical expectations derived from bifurcation and phase space analysis. These experimental observations validate the dynamic richness and controllability of the implemented chaotic system.

The strong agreement between the experimental and simulated results underscores the accuracy and fidelity of the implemented model. The phase portraits and state trajectories captured by the oscilloscope not only replicate the expected dynamical features but also provide empirical evidence of the system's nonlinear oscillatory regime. Moreover, these observations corroborate the theoretical analysis of the chaotic system, which predicts the emergence of multiple-scroll attractors under a varying bifurcation control parameter. The experimentally observed topological patterns align with the mathematical formulations, demonstrating that the proposed system exhibits structurally rich dynamics that are both self-excited and parameter-dependent.

In conclusion, the congruence between simulation and hardware-based experimental results confirms the validity and practicality of deploying chaotic systems using PLC platforms. This research substantiates that real-time chaotic behavior, including multi-scroll attractors and complex self-excited dynamics, can be faithfully reproduced within an industrial control environment. These results not only reinforce the theoretical underpinnings of the system's nonlinear dynamics but also open avenues for leveraging chaos in real-world applications such as secure communications, random number generation, and intelligent control in IIoT systems.

Dynamics 2025, 5, 40 17 of 20

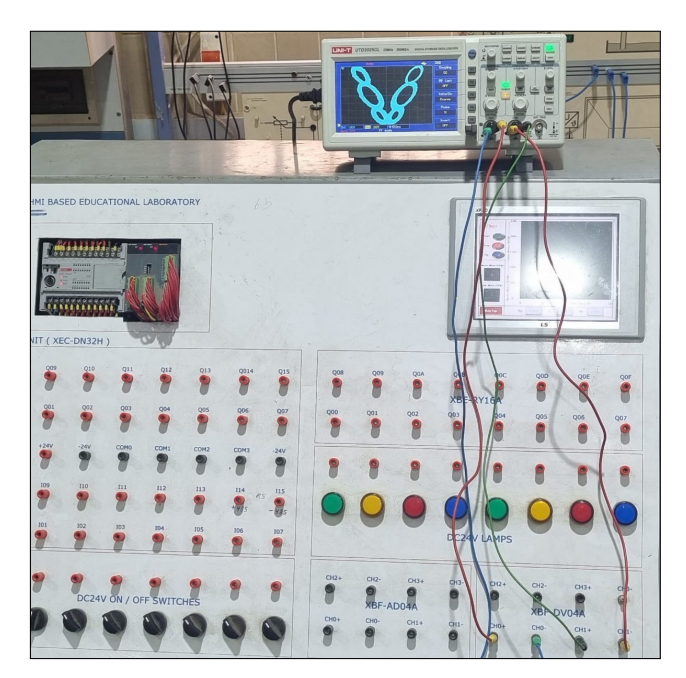


**Figure 18.** Hardware setup of (XEC-DN32H) PLC with the (XBF-DV04A) analogue output expansion module to implement V/Heart-shape chaotic system (1).

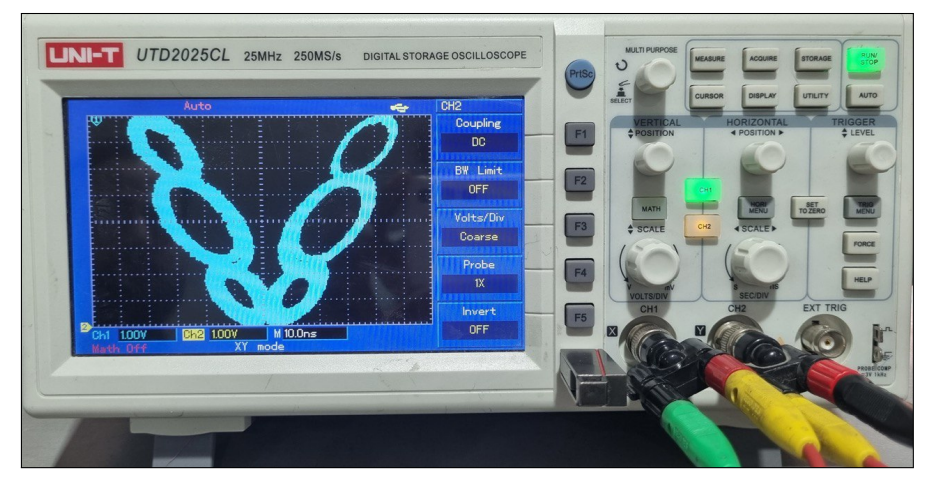


**Figure 19.** Two-dimensional phase portrait for V/Heart-shape chaotic system (1) when  $m_1 = 1$ .

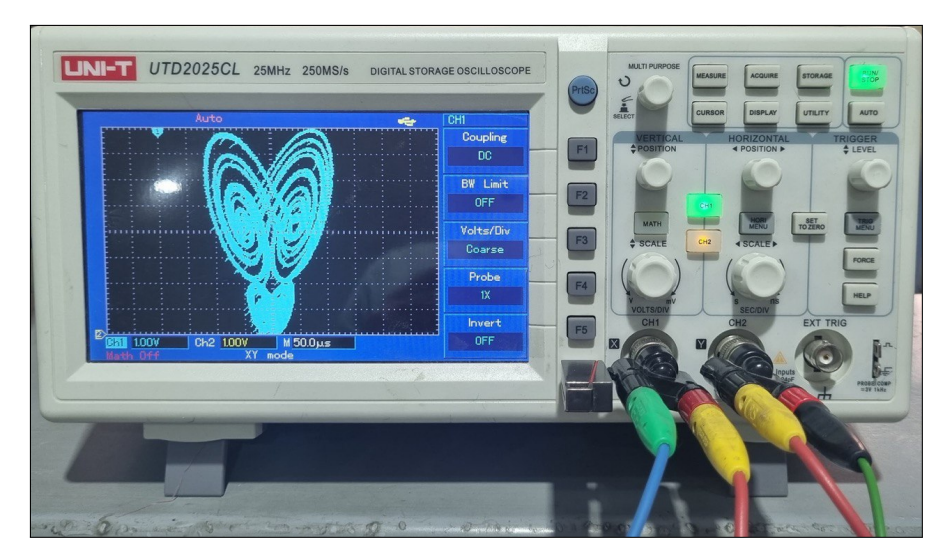


**Figure 20.** Two-dimensional phase portrait for V/Heart-shape chaotic system (1) when  $m_1 = 2$ .

Dynamics 2025, 5, 40 18 of 20

## 5. Conclusions

In conclusion, this study successfully explores the nonlinear dynamics and practical implementation of a V/Heart-shape chaotic system. The system was designed and realized using an industrial-grade programmable logic controller (PLC) with structured text (ST) language, ensuring reliable hardware execution. Through the application of nonlinear analysis tools, such as bifurcation diagrams, Lyapunov exponents, and phase portraits, the intricate dynamical behaviors of the system were comprehensively analyzed. The versatility of the proposed system was demonstrated through two case studies involving parameter variations, which revealed distinct phenomena including self-excited, hidden, and coexisting attractors. The results of simulations of the chaotic dynamics closely matched experimental results obtained from laboratory hardware implementations, underscoring the system's accuracy and practicality. These findings emphasize the significant potential of the proposed chaotic system for a wide range of applications, including secure communications, advanced industrial systems, and dynamic system analyses. As a direction for future work, we propose the realization of chaotic systems using programmable logic controllers (PLCs) as a means to enhance edge computing capabilities within IIoT environments. The intrinsic properties of chaotic systems—such as high sensitivity to initial conditions and pseudorandom behavior—can be harnessed for advanced functionalities, including secure data encryption, real-time anomaly detection, and robust sensor data validation. Implementing these systems on PLCs, which serve as industrial edge devices, facilitates decentralized processing and decision-making closer to the physical layer. This reduces reliance on cloud computing resources, minimizes network latency, and increases system resilience—key requirements for time-critical IIoT applications such as predictive maintenance, smart manufacturing, and autonomous process control. Additionally, the integration of these PLC-based chaotic modules with IIoT middleware—such as edge gateways, digital twins, and industrial protocols like OPC UA and MQTT—will be explored to ensure seamless data flow and interoperability across distributed cyber-physical systems.

**Author Contributions:** Conceptualization, A.-B.A.A.-H.; formal analysis, H.A.A.; investigation, H.A.A.; methodology, A.-B.A.A.-H.; software, F.R.T.; supervision, V.-T.P.; validation, F.R.T.; visualization, M.M.A.; writing—original draft, M.M.A.; writing—review and editing, V.-T.P. All authors have read and agreed to the published version of the manuscript.

Funding: This research received no external funding.

**Data Availability Statement:** The authors declare that the data supporting the findings of this study are all available within the article.

Conflicts of Interest: The authors have declared no conflicts of interest.

#### **Abbreviations**

The following abbreviations are used in this manuscript:

CORDIC Coordinate rotation digital computer

CPU Central processing uni
DAC Digital-to-analogue converter
DSP Digital signal processing
FPGA Field-programmable gate array

GL Grünwald–Letnikov

IIoT Industrial Internet of ThingsMQTT Message Queuing Telemetry Transport

OPC UA Open Platform Communications Unified Architecture

PLC Programmable logic controller

Dynamics 2025, 5, 40 19 of 20

PSD Power spectral density

SCADA Supervisory control and data acquisition

SE Spectral entropy

ST Structured text language
UDFBs User-defined function blocks

#### References

1. Strogatz, S.H. Nonlinear Dynamics and Chaos: With Applications to Physics, Biology, Chemistry, and Engineering (Studies in Nonlinearity); Westview Press: Boulder, CO, USA, 2001; Volume 1.

- 2. Lorenz, E.N. Deterministic nonperiodic flow. J. Atmos. Sci. 1963, 20, 130–141. [CrossRef]
- 3. Cheffer, A.; Savi, M.A. Biochaos in cardiac rhythms. Eur. Phys. J. Spec. Top. 2022, 231, 833–845. [CrossRef]
- 4. Kargarnovin, S.; Hernandez, C.; Farahani, F.V.; Karwowski, W. Evidence of Chaos in Electroencephalogram Signatures of Human Performance: A Systematic Review. *Brain Sci.* **2023**, *13*, 813. [CrossRef]
- 5. Al-Hussein, A.B.A.; Tahir, F.R.; Rajagopal, K. Chaotic Power System Stabilization Based on Novel Incommensurate Fractional-Order Linear Augmentation Controller. *Complexity* **2021**, 2021, 3334609. [CrossRef]
- 6. Wang, M.; Yi, Z.; Li, Z. A memristive Ikeda map and its application in image encryption. *Chaos Solitons Fractals* **2025**, *190*, 115740. [CrossRef]
- 7. Al-Hussein, A.B.A.; Tahir, F.R.; Al-Suhail, G.A. Design and FPGA Implementation of a Hyper-Chaotic System for Real-Time Secure Image Transmission. *Iraqi J. Electro. Eng.* **2025**, *21*, 55–68. [CrossRef]
- 8. Soliman, N.S.; Tolba, M.F.; Said, L.A.; Madian, A.H.; Radwan, A.G. Fractional X-shape controllable multi-scroll attractor with parameter effect and FPGA automatic design tool software. *Chaos Solitons Fractals* **2019**, 126, 292–307. [CrossRef]
- 9. Clemente-López, D.; Munoz-Pacheco, J.M.; Rangel-Magdaleno, J.d.J. A review of the digital implementation of continuous-time fractional-order chaotic systems using FPGAs and embedded hardware. *Arch. Comput. Methods Eng.* **2023**, *30*, 951–983. [CrossRef]
- 10. Vaidyanathan, S.; Tlelo-Cuautle, E.; Benkouider, K.; Sambas, A.; Ovilla-Martínez, B. FPGA-based implementation of a new 3-D multistable chaotic jerk system with two unstable balance points. *Technologies* **2023**, *11*, 92. [CrossRef]
- Mohamed, S.M.; Sayed, W.S.; Madian, A.H.; Radwan, A.G.; Said, L.A. An encryption application and FPGA realization of a fractional memristive chaotic system. *Electronics* 2023, 12, 1219. [CrossRef]
- 12. Guo, Z.; Wen, J.; Mou, J. Dynamic analysis and DSP implementation of memristor chaotic systems with multiple forms of hidden attractors. *Mathematics* **2022**, *11*, 24. [CrossRef]
- 13. Wang, X.; Feng, Y.; Chen, Y. A new four-dimensional chaotic system and its circuit implementation. *Front. Phys.* **2022**, *10*, 906138. [CrossRef]
- 14. Yau, K.; Chow, K.P. PLC forensics based on control program logic change detection. *J. Digit. Forensics Secur. Law* **2015**, *10*, 5. [CrossRef]
- 15. Homay, A.; de Sousa, M.; Wollschlaeger, M. Chaotic Pendulum in Industrial Control and Automation Software. In Proceedings of the 2024 IEEE 22nd International Conference on Industrial Informatics (INDIN), Beijing, China, 18–20 August 2024; pp. 1–6.
- 16. Abou-Bakr, E.; Alnajim, A.M.; Alashwal, M.; Elmanfaloty, R.A. Chaotic sequence-driven path planning for autonomous robot terrain coverage. *Comput. Electr. Eng.* **2025**, *123*, 110032. [CrossRef]
- 17. Pal, P.; Parvathy, A.; Devabalaji, K.; Antony, S.J.; Ocheme, S.; Babu, T.S.; Alhelou, H.H.; Yuvaraj, T. IoT-based real time energy management of virtual power plant using PLC for Transactive energy framework. *IEEE Access* **2021**, *9*, 97643–97660. [CrossRef]
- 18. Alabadi, M.; Habbal, A.; Wei, X. Industrial internet of things: Requirements, architecture, challenges, and future research directions. *IEEE Access* **2022**, *10*, 66374–66400. [CrossRef]
- 19. Zidan, M.A.; Radwan, A.G.; Salama, K.N. Controllable V-shape multiscroll butterfly attractor: System and circuit implementation. *Int. J. Bifurc. Chaos* **2012**, 22, 1250143. [CrossRef]
- 20. Shahhosseini, A.; Tien, M.H.; D'Souza, K. Poincare maps: A modern systematic approach toward obtaining effective sections. *Nonlinear Dyn.* **2023**, *111*, 529–548. [CrossRef]
- 21. Wolf, A.; Swift, J.B.; Swinney, H.L.; Vastano, J.A. Determining Lyapunov exponents from a time series. *Phys. D Nonlinear Phenom.* **1985**, *16*, 285–317. [CrossRef]
- 22. Sun, K. Chaotic Secure Communication: Principles and Technologies; Walter de Gruyter GmbH & Co KG: Berlin, Germany, 2016.
- 23. Moussa, K.H.; El Naggary, A.I.; Mohamed, H.G. Non-Linear Hopped Chaos Parameters-Based Image Encryption Algorithm Using Histogram Equalization. *Entropy* **2021**, 23, 535. [CrossRef]
- 24. Malik, D.S.; Shah, T. Color multiple image encryption scheme based on 3D-chaotic maps. *Math. Comput. Simul.* **2020**, *178*, 646–666. [CrossRef]
- 25. He, N.; Oke, V.; Allen, G. Model-based verification of PLC programs using Simulink design. In Proceedings of the 2016 IEEE International Conference on Electro Information Technology (EIT), Grand Forks, ND, USA, 19–21 May 2016; pp. 0211–0216.

Dynamics 2025, 5, 40 20 of 20

26. Ovatman, T.; Aral, A.; Polat, D.; Ünver, A.O. An overview of model checking practices on verification of PLC software. *Softw. Syst. Model.* **2016**, *15*, 937–960. [CrossRef]

- 27. LS Electric Co., Ltd. Catalog for LS XGB XEC-DN32H PLC Series. 2025. Available online: https://sol.ls-electric.com/ww/en/product/document/1263 (accessed on 1 August 2025).
- 28. LS Electric Co., Ltd. XBF-DV04A DAC Module English Manual V1.8. 2024. Available online: https://sol.ls-electric.com/ww/en/product/document/2427 (accessed on 1 August 2025).
- 29. Abdulkareem, H.; Rahma, F.; Radhi, J. Liquid Mixing Enhancement by PLC-Based Chaotic Dynamics Implementation. *Iraqi J. Electr. Electron. Eng.* **2019**, 15, 10–20. [CrossRef]

**Disclaimer/Publisher's Note:** The statements, opinions and data contained in all publications are solely those of the individual author(s) and contributor(s) and not of MDPI and/or the editor(s). MDPI and/or the editor(s) disclaim responsibility for any injury to people or property resulting from any ideas, methods, instructions or products referred to in the content.